ОБЪЕДИНЕННЫЙ
ИНСТИТУТ
ЯДЕРНЫХ
ИССЛЕДОВАНИЙ

Дубна

E1 - 3707

Z.Janout, Yu.M.Kazarinov, F.Lehar,
A.M.Rozanova

UNAMBIGUOUS PHASE SHIFT ANALYSIS OF NUCLEON-NUCLEON SCATTERING AT 400 MeV AND THE ENERGY DEPENDENCE OF PHASE SHIFTS ABOVE THE PION PRODUCTION THRESHOLD

ЛАБОРАТОРИЯ ЯДЕРНЫХ ПРОБЛЕМ

1968

=2 м

Яноут З., Казаринов Ю.М., Легар Ф., Розанова А.М. E1-3707

Однозначный фазовый анализ нуклон-нуклонного рассеяния при энергии 400 Мэв и энергетическая зависимость фазовых сдвигов выше порога мезонообразования.

Выполнен фазовый анализ данных по рассеянию нуклонов нуклонами при энергиях, близких к 400 Мэв. Поиск наборов фазовых сдвигов производился при максимальном орбитальном моменте $\ell_{max} = 4$ с одной мнимой добавкой к фазовому сдвигу волны $^1D_2$. При значениях $\chi^2 \le 1,5 \bar{\chi}^2$ найдено семь решений. Исследование показало, однако, что шесть из них могут быть отброшены с вероятностью ошибки первого рода меньше 0,59 %.

Приведены таблицы фазовых сдвигов и расчетные угловые зависимости экспериментальных величин. Даны энергетические зависимости фазовых сдвигов в интервале энергий от 10 до 630 Мэв.

Препринт Объединенного института ядерных исследований.
Дубна, 1968.

Janout Z., Kazarinov Yu.M., Lehar F., Rozanova A.M. E1-3707

Unambiguous Phase Shift Analysis of Nucleon-Nucleon Scattering at 400 MeV and the Energy Dependence of Phase Shifts Above the Pion Production Threshold

The phase shift analysis of Nucleon-Nucleon scattering data at energies near 400 MeV has been performed. The search for the solutions of the phase shifts has been carried out for the maximal orbital momentum $\ell_{max} = 4$. Only the $^1D_2$ wave is assumed to have an immaginary part. Seven solutions have been obtained in the region $\chi^2 \le 1.5 \bar{\chi}^2$. A detailed investigation has shown, that six of them can be rejected with the probability of Type I error smaller than 0.59 %.

Tables of phase shifts and the angular dependences of the experimental quantities are given. The energy dependences of phase shifts in the region 10-630 MeV are shown in the graphs.

Preprint. Joint Institute for Nuclear Research.
Dubna, 1968

E1 - 3707

Z.Janout, Yu.M.Kazarinov, F.Lehar,
A.M.Rozanova

UNAMBIGUOUS PHASE SHIFT ANALYSIS OF NUCLEON–NUCLEON SCATTERING AT 400 MeV AND THE ENERGY DEPENDENCE OF PHASE SHIFTS ABOVE THE PION PRODUCTION THRESHOLD

Submitted to Nuclear Physics

Introduction

The first simultaneous phase shift analysis of $n-p$ and $p-p$ data at 400 MeV was performed previously in ref.[1]. The search for solutions from random initial conditions was carried out for the maximal orbital momentum $\ell_{max} = 3$, i.e. the phase shifts for states with $\ell \leq 3$ were found from experimental data and the interaction in the higher states was taken into account in the one - pion exchange approximation. However, none of the previously obtained sets did not describe sufficiently the experimental data used for the phase shift analysis and therefore, all the found solutions were specified for $\ell_{max} = 4$. Then, a reasonable description of the experimental data was obtained [1]. Latter, the three solutions found in [1] were specified using additional new experimental data [2]. Only the first and fourth solutions remained (sets 1 and 2 coincided).

In the last few years a considerable amount of new experimental data at energies near 400 MeV was obtained, namely the polarization and spin correlation in $p-p$ elastic scattering were measured, using a polarized proton target [3]. The quantities P_{np} and P_{pp} were also measured at 400 MeV in double scattering experiments[4].

Results of these experiments together with the previously known data are used in this paper to determine the phase shifts more accurately and to investigate unambiguity of the phase shift analysis with $\ell_{max}=4$, i.e. in the conditions which are necessary for a sufficient description of experimental data.

2. Experimental Data

The experimental quantities used in the phase shift analysis are given in Table 1. Unfortunately the total number of experimental points equal to 149 is not distributed uniformly between the $p-p$ and $n-p$ systems. The $p-p$ data (120 points) were measured well accurately and lie in the energy region 380-437 MeV. The differential cross section for $n-p$ scattering and the polarization P_{np} were measured at 400 MeV. The "averaging" of the experimental data over such an energy region and their reduction to one energy should not influence the results of the phase shift analysis, since the angular distributions of the experimental quantities only slightly depend on the energy in the region considered. All the experimental data are given in Table 2.

3. Phase Shift Analysis

The search for random initial parameters was performed according to the programme decribed in [5]. As many as 170 searches were performed and 7 solutions with $\chi^2 < 1.5 \ \bar{\chi}^2$ were found. On the basis of 149 experimental points, 23 variable parameters for $\ell_{max} = 4$ were determined ($\chi^2 = 126$) . The values of the phase shifts and of χ^2 for the first five sets are given in Table 3. For the sixth and seventh solutions the χ^2 values are equal to 158.7 and 181.6, respectively. The first set with the minimal χ^2 value corresponds to set 1 obtained previously in [1,2].

Since a great number of sets has been found, it was interesting to try to exclude some of the solutions with the help of existing statistical criteria. For this reason the probability $P(\chi^2 \geq \chi_i^2)$ of the appearence of the χ^2 value, which is larger or equal to χ_i^2, arising in the phase shift analysis, was calculated for all sets(1,..7). This probability proved equal to 73.2, 52,8, 19.0, 18.7, 17.1, 2.6 and 0.1%, respectively. It follows from the found values of $P(\chi^2 \geq \chi_i^2)$, that only solutions 6 and 7 can be rejected according to the χ^2 criterion, because their probabilities $P(\chi^2 \geq \chi_i^2)$ are small.

A method suggested in [6] was used to estimate the probability of an Type I error in order to discriminate between the remaining solutions. All the solutions are compared with set 1, which have the minimal χ^2 value. This set was taken as the model of the real solution.

According to ref. [6] for the calculation of the majorized estimation of Type I error probability P_i it is necessary to model the repeating of the experiment (pseudoexperiment). It was made using the Monte Carlo method and P_i can be expressed by the formula:

$$P_i = \frac{1}{N} \sum_{j=1}^{N} P_{ij} \, (\Delta \geq \Delta_i' - \delta_{ij}), \quad i = 2, \ldots, 7, \qquad (1)$$

where N is the number of pseudoexperiments, P_{ij} the probabilities of the Type I error for the j -th pseudoexperiment.

$$P_{ij}(\Delta \geq \Delta_i' - \delta_{ij}) = 1, \quad \text{if} \quad \Delta_i' - \delta_{ij} < 0,$$

$$P_{ij}(\Delta \geq \Delta_i' - \delta_{ij}) = \frac{1}{2}(1 - \phi(\sqrt{\Delta_i' - \delta_{ij}})), \quad \text{if} \quad \Delta_i' - \delta_{ij} \geq 0, \tag{2}$$

$\phi(\sqrt{\Delta_i' - \delta_{ij}})$ is the integral of error, $\Delta_i' = \chi_i^2 - \chi_1^2 (i = 2,..7)$ is the difference between the χ^2 values of i -th and first solutions, obtained in the phase shift analysis $\delta_{ij} = \chi_{ij}^2 - \chi_{1j}^2$ is the χ^2 difference of the i -th and first solution, realized in j -th pseudoexperiment.

In view of time sparing the probabilities P_{ij} are determined for the linearized hypotheses /6/. For this reason the quantities $\gamma_{jk}\sigma_k$ were used as the experimental data after j -th pseudoexperiment. Here σ_k is the standart deviation of the k -th point, γ_{jk} are the random numbers, in the region $-4 \leq \gamma_{jk} \leq 4$ satisfying the Gauss distribution law with unity dispersion. In our case 103, 103, 34, 31, 25, 25, 25 pseudoexperiments were performed for sets 1-7, respectively. The number of pseudoexperiments N depends on the accuracy, to which we wish to determine the probability of the Type I error.

The majorized estimation of the probability of the Type I error was obtained $P_I = (0.59 \pm 0.06)\%$ for the second set and is smaller than $5 \cdot 10^{-4}\%$ for all other sets. Since in all the cases the calculations were performed using a linearized hypotheses, the value P_I is the upper limit of the probability estimation.

From this results it follows, that, on the basis of this method only the first solution of 400 MeV phase shift analysis remain and all other solutions can be rejected. Then the phase shift analysis at 400 MeV, can be considered to be unambiguous at present.

The measurement of new experimental data and increasing of the accuracy of the previously known values make it necessary the specifying of the phase shift analysis solutions at higher values of ℓ_{max}, i.e. to increase the number of phase shifts for satisfying description of experimental data. It was interesting to prove the specification of the remaining solution [x)] for $\ell_{max}=5$. The phase shifts for $\ell_{max}=5$ are shown in Table 4. It follows from the table that the mean values of the phase shifts are not changed, but their errors are essentially increased, mainly for the phase shifts with the isospin $T=0$ ($^3S_1$, $^1P_1$, ϵ_1, $^3D_2$, $^3G_3$, $^3G_4$).

The unambiguous result of the phase shift analysis at 400 MeV makes it possible, to extrapolate the energy dependences of the phase shifts up to 700 MeV. Now we can decide which of the two phase shift sets at 630 MeV is better described by curves extrapolated from the low energy region. For this reason the results of the phase shift analysis at 9.7, 14.5, 18.2, 23.1, 40, 52, 66, 95, 147, 210, 310, 630 /7,8/ and the present result are used. The energy dependence of each phase shift can be approximated by the formula

$$\delta(E) = \sum_{i=0}^{m} a_i k^i , \qquad (3)$$

where $k=\sqrt{E}$, E is the energy in the lab. system. The coefficient a_0 is taken to be equal to 180° for the phase shift of the $^3S_1$ wave and to be zero for all other waves except $^1S_0$. For the $^1S_0$ wave the region 0–10 MeV is not taken into account. The coefficients a_i were determined using the least squares method and are given in Table 5. The number of coefficients was chosen

---

x) The specification of the second solution at transition to $\ell_{max}=5$ gives the same result as that of the first solution.

using the criterion, that the increasing of the coefficients gives not a better description of the phase shifts energy dependence. It was found that 3-4 coefficients give a good description. The energy dependences $\delta(E)$ are given in figs. 1-6. In the same figures the phase shifts are shown, obtained from the energy independent phase shift analysis (see refs. /7,8/). From the graphs it follows, that all the curves in the region 400-700 MeV can be well extrapolated from the low energy region. It can be stated, that the third phase shift set at 630 MeV better coincides with the extrapolated curves than the second one. For 630 MeV the values of the third phase shift set are taken into account /7/. If the curves for second and third solution considerably differ, both the dependences are given.

The following parameters do not coincide with the calculated curves: Phase shifts $^3G_4$ at 400 MeV and $^3F_4$ at 147 MeV, the mixing parameter ϵ_1 at 310 MeV and due to $^3S_1$ and $^3D_1$ at the same energy. The investigation of the χ^2 profile at 400 MeV shows, that in all cases only one minimum exists (fig. 7).

4. Results

In the phase shift analysis of the nucleon - nucleon scattering data near 400 MeV, seven solutions for $\ell_{max}=4$ (23 free parameters) were found in the region $\chi^2 \leq 1.5\bar{\chi}^2$. The majorized estimation of the probability Type I error by rejecting each of this solutions shows, that the solutions 2-7 can be rejected with probability of 0.59% from the second set and smaller than $5 \cdot 10^{-4}$ % for all other sets.

The known experimental data, used in the phase shift analysis are well described at $\ell_{max}=4$ ($\chi^2/\bar{\chi}^2 = 0.91$). For $\ell_{max}=5$ (28 free parameters) the description of experimental data is not improved

($\chi^2/\bar{\chi}^2 \approx 0.94$). The mean values of the phase shifts are changed within the errors by this tranzition.

The obtained phase shifts at 400 MeV well coincide with calculated curves $\delta(E)$, obtained on the basis of the energy independent phase shift analysis data in the region 9.7 - 630 MeV. The energy dependences $\delta(E)$ obtained in Livermore /9/ for the phase shifts of waves with isospin $T = 1$ in the energy dependent phase shift analysis are consistent with our results.

The angular dependences of experimental values calculated at 400 MeV on the basis of the 1-st phase shift set (see figs. 8-13) are in good agreement with the analogous dependences at 310 MeV. In fig.8 the angular dependences of C^{pp}_{nn} for the 1-st and 2-nd sets at 400 MeV are given. In this case the experimental data are better described by the 2-nd set ($\Delta \chi^2 = 9.5$ for the 2-nd set and 15.00 for the 1-st set).

The $\pi - N$ coupling constant f^2 calculated for all the phase shift sets at 400 MeV coincide with the f^2 value obtained in the $\pi - p$ scattering measurements within the errors.

The accuracy of the phase shifts for $T = 0$ is considerably lower that that for $T = 1$. In view of this fact the accurate measurements of the $n - p$ quantities are desirable.

The authors express their deep gratitude to N.A.Booth for sending us the interesting data, L.I.Lapidus and P.Winternitz for useful discussions, E.Dudova, V.A.Maximova, J.Cechova , J.Fingerova and L.Janoutova for help in the work.

References

1. Ю.М.Казаринов, В.С.Киселев, Ю.Н.Симонов. ЯФ, 2, 1095 (1965).

2. Ю.М.Казаринов, Ф.Легар, З.Яноут. Письма в ЖЭТФ, 4, 110 (1966).

3. A.Beretvas, N.E.Both , C.Dolnick, R.J.Esterling, R.E.Hill, J.Scheid, D.Sherden, A.Yokosawa. Report 410, University, Chicago 1967.

4. D.Cheng. Rev. Mod. Phys., 39, 526 (1967).

5. Ю.М.Казаринов, И.Н.Силин. ЖЭТФ, 43, 692 (1962).

6. Ю.М.Казаринов, В.С.Киселев, А.М.Розанова, И.Н.Силин. Препринт ОИЯИ, Р1-3268, 1967.

7. Л.И.Глонти, Ю.М.Казаринов, А.М.Розанова, И.Н.Силин. Препринт ОИЯИ, Р1-3525, 1967.

8. Yu.M.Kazarinov, F.Lehar, Z. Janout, Rev. Mod. Phys., 39, 571 (1967). Z.Janout, Yu.M.Kazarinov, F.Lehar, Preprint E1-2952, Dubna , 1966.
Ю.М.Казаринов, Ф.Легар., З.Яноут. ЯФ, 6, 174 (1967).

Z.Janout, Yu.M.Kazarinov, F.Lehar, P.Winternitz, Preprint E1-3345, Dubna, 1967.

Ю.М.Казаринов, В.С.Киселев, Ю.Н.Симонов. Препринт ОИЯИ, Р-2241, 1965.

9. M.H.MacGregor , R.A.Arndt, R.M.Wright. Preprint UCRL 70075, Livermore 1967.

10. D.Harting, J.R.Holt, J.A.Moore. Proc. Phys. Soc., 71, 770 (1958).

11. J.R.Holt, J.C.Kluyver, J.A.Moore. Proc. Phys. Soc., 71, 781(1958).

12. R.B.Sutton, T.H.Fields, J.G.Fox., J.A.Kane, W.E.Mott, R.A.Stallwood. Phys. Rev., 97, 783 (1955).

13. J.A.Kane, R.A.Stallwood, R.B.Sutton, T.H.Fields, J.G.Fox., Phys. Rev., 95, 1694 (1954).

14. R.Roth, E.Engels, S.C.Wright, P.Kloeppel, R.Handler, L.G.Pondrom. Phys. Rev., 140, B1533 (1965).

15. J.A.Kane, R.A.Stallwood, R.B.Sutton, J.G.Fox. Bull. Amer. Phys. Soc., 1, 9, (1956).

16. J.V.Allaby, A.Ashmore, A.N.Diddens, J.Eades, G.B.Huxtable,

K.Skarsvag. Proc. Phys. Soc., 77, 234, (1961).

17. E.Engels. , T.Bowen, J.W.Cronin, R.L.McIlwain, L.G.Pondrom. Phys,. Rev., 129, 185[illegible] (1963).

18. V.P.Dzhelepov, V.I.Moskalev, S.V.Medved. Dokl. Akad. Nauk., 140, 380 (1965).

19. A.J.Hartzler, R.T.Siegel, W.Opitz. Phys. Rev., 95, 591 (1954).
A.J.Hartzler, R.T.Siegel. Phys. Rev., 95, 185 (1954).

20. V.A.Nedzel. Phys. Rev., 94, 174 (1954).

Received by Publishing Department
on February 13, 1968.

Table 1

The Experimental Data, Used in Phase Shift Analysis at 400 MeV

Measured Quantity	Energy /MeV/	Angular Range /CM/	Number of Points	$\Delta\chi^2$ +)	Authors	Refs.
σ^{pp}	380	4°–31°	20	4.80	Harting et al	/10/
	380	30°–90°	6	5.26	Holt et al.	/11/
	437	17°–90°	8	4.26	Sutton et al.	/12/
P_{pp}	400	33°–83°	7	3.40	Cheng	/4/
	415	52°–88°	14	9.18	Beretvas et al.	/3/
	415	15°–90°	8	10.17	Kane et al.	/13/
	430	30°–120°	7	7.19	Roth et al.	/14/
D_{pp}	415	90°	1	2.07	Kane et al.	/15/
	430	30°–120°	7	4.19	Roth et al.	/14/
R_{pp}	430	30°–120°	7	3.12	Roth et al.	/14/
A_{pp}	430	30°–120°	7	14.46	Roth et al.	/14/
A'_{pp}	430	30°–120°	7	15.84	Roth et al.	/14/
C^{pp}_{nn}	382	90°	1	0.004	Allaby et al.	/16/
	400	60°, 90°	2	4.15	Engels et al.	/17/
	415	52°–90°	15	15.00	Beretvas et al.	/3/
C^{pp}_{ml}	400	60°, 90°	2	0.61	Engels et al.	/17/
σ^{pp}_t	410		1	0.39	Dzhelepov et al	/18/
σ^{np}	400	12°–180°	20	9.94	Hartzler et al.	/19/
P_{pn}	400	33°–144°	8	1.63	Cheng	/4/
σ^{np}_t	410		1	0.01	Nedzel	/20/

+) The contribution to χ^2 for the 1-st set.

Table 2

The Experimental Data Used in Phase - Shift Analysis for pp- and np- Scattering at Energy 400 MeV.

Parameter	Energy MeV	$\vartheta^o_{c.m.s.}$	Measured value	Statistical error ±	Refs.
			$\left(\frac{d\sigma}{d\Omega}\right)_\vartheta \Big/ \left(\frac{d\sigma}{d\Omega}\right)_{90^o}$		
σ_{pp} *)	380	30	1.092	0.010	/11/
		36	1.092	0.014	
		43	1.082	0.010	
		50	1.045	0.012	
		65	1.023	0.012	
		90	1.000	0.006	
	380	4.14	7.07	0.30	/10/
		4.69	4.26	0.17	
		5.28	3.08	0.12	
		6.42	1.783	0.054	
		7.56	1.435	0.040	
		8.73	1.238	0.028	
		9.9	1.176	0.027	
		11.0	1.176	0.020	
		12.1	1.173	0.027	
		13.2	1.165	0.015	
		14.3	1.176	0.022	
		15.4	1.151	0.018	
		16.5	1.154	0.016	
		17.6	1.154	0.015	
		19.8	1.133	0.020	
		21.8	1.141	0.016	
		24.0	1.114	0.016	
		26.2	1.130	0.018	
		28.4	1.103	0.017	
		30.6	1.084	0.017	

*) Differential cross section are given in terms of the value at 90°.

$$\left(\frac{d\sigma}{d\Omega}\right)_{90^o c.m.s.} = (3.70 \pm 0.06) \text{ mb/sterad}$$

Parameter	Energy MeV	$\vartheta^{o}_{c.m.s.}$	Measured value	Statistical error ±	Refs.
			$\left(\frac{d\sigma}{d\Omega}\right)_{\vartheta} \Big/ \left(\frac{d\sigma}{d\Omega}\right)_{90^o}$		
σ_{pp} *)	437	17	1.182	0.035	/12/
		25	1.223	0.023	
		28	1.156	0.031	
		30	1.152	0.015	
		36	1.160	0.010	
		50	1.014	0.015	
		65	1.037	0.017	
		90	1.000	0.014	
P_{pp}	415	15.5	0.317	0.041	/13/
		22	0.353	0.027	
		33	0.421	0.036	
		43.5	0.402	0.029	
		55.5	0.317	0.028	
		65	0.260	0.030	
		75	0.117	0.021	
		90	-0.017	0.023	
	415	52.0	0.39	0.03	/ 3/ **)
		55.0	0.38	0.03	
		58.5	0.30	0.03	
		63.0	0.28	0.03	
		65.7	0.23	0.03	
		69.6	0.20	0.03	
		74.0	0.16	0.03	

*) Differential cross section are given in terms of the value at 90°.

$$\left(\frac{d\sigma}{d\Omega}\right)_{90^o c.m.s.} = (3.49 \pm 0.17)\ \text{mb/sterad.}$$

**) This data were taken from the graph (see ref. /3/).

Table 2 - Continuation

Parameter	Energy MeV	$\vartheta^o_{c.m.s.}$	Measured value	Statistical error ±	Refs.
P_{pp}	415	78.5	0.09	0.03	/ 3/
		81.5	0.08	0.03	
		82.3	0.09	0.03	
		83.1	0.07	0.03	
		86.2	0.06	0.03	
		87.0	0.01	0.02	
		88.0	0.03	0.03	
	430	30	0.33	0.06	/14/
		45	0.40	0.06	
		60	0.25	0.04	
		75	0.16	0.03	
		90	0.00	0.02	
		105	-0.23	0.05	
		120	-0.40	0.11	
D_{pp}	415	90	0.42	0.09	/15/
	430	30	0.34	0.22	/14/
		45	0.60	0.19	
		60	0.47	0.13	
		75	0.52	0.11	
		90	0.67	0.10	
		105	0.65	0.15	
		120	0.59	0.25	
R_{pp}	430	30	0.06	0.11	/14/
		45	0.40	0.11	
		60	0.43	0.08	
		75	0.47	0.07	
		90	0.47	0.05	
		105	0.35	0.11	
		120	0.34	0.18	

Table 2 - Continuation

Parameter	Energy MeV	$\vartheta^o_{c.m.s.}$	Measured value	Statistical error $\pm$	Refs.
A_{pp}	430	30	0.25	0.16	/14/
		45	-0.15	0.12	
		60	0.36	0.09	
		75	0.35	0.08	
		90	0.27	0.07	
		105	-0.12	0.16	
		120	-0.12	0.22	
A'_{pp}	430	30	0.47	0.20	/14/
		45	0.06	0.11	
		60	0.06	0.09	
		75	0.22	0.08	
		90	0.36	0.07	
		105	0.01	0.11	
		120	0.08	0.04	
C^{pp}_{nn}	382	90	0.41	0.09	/16/
	400	50	0.82	0.47	/17/
		90	0.60	0.09	
	415	52.0	0.60	0.07	/3/ *)
		55.0	0.58	0.06	
		58.5	0.56	0.06	
		63.0	0.51	0.05	
		65.7	0.49	0.05	
		69.6	0.47	0.05	
		74.0	0.54	0.05	
		78.5	0.35	0.05	
		81.5	0.48	0.05	
		82.3	0.40	0.05	
		83.1	0.48	0.05	
		86.2	0.41	0.05	
		87.0	0.42	0.05	
		88.0	0.44	0.05	
		90.0	0.42	0.04	

*) This data were taken from the graph (see ref. /3/).

Table 2 - Continuation

Parameter	Energy MeV	$\vartheta^o_{c.m.s.}$	Measured value	Statistical error ±	Refs.
C^{pp}_{ml}	400	60	0.60	0.46	/17/
		90	0.32	0.09	
σ^{t}_{pp} mb	410	0.01	26.9	0.7	/18/
σ_{np}	400	12.7	3.73	2.10	/19/
		15	4.43	0.46	
mb/sterad		20	3.07	0.37	
		30	2.84	0.57	
		40	3.33	0.20	
		45	3.35	0.20	
		50	3.38	0.12	
		55	2.56	0.23	
		60	2.48	0.08	
		70	2.22	0.09	
		80	1.85	0.06	
		90	1.54	0.06	
		100	1.42	0.06	
		110	1.50	0.08	
		120	1.94	0.08	
		130	2.50	0.09	
		140	3.21	0.09	
		150	4.17	0.11	
		160	5.25	0.14	
		165	5.82	0.22	
		170	7.93	0.28	
		175	9.57	0.34	
		180	13.49	0.91	

Parameter	Energy MeV	ϑ^{o} cms	Measured Value	Statistical error ±	Refs.
P_{pp}	400	33.8	0.442	0.014	/4/
		47.8	0.419	0.008	
		48.0	0.419	0.011	
		63.5	0.275	0.008	
		65.2	0.272	0.010	
		80.6	0.105	0.008	
		82.5	0.084	0.009	
P_{pn}	400	33.1	0.411	0.087	/4/
		48.3	0.264	0.023	
		66.6	0.083	0.032	
		83.1	-0.152	0.026	
		99.7	-0.309	0.025	
		116.5	-0.272	0.022	
		131.1	-0.158	0.018	
		144.3	-0.104	0.056	
σ^{t}_{np} /mb/	410		33.7	1.3	/20/

Table 3 The Phase-Shifts in Degrees (the Stapp parametrization) for 400 MeV Nucleon-Nucleon Scattering

Phase Shifts	$\delta \pm \Delta\delta$	$\delta \pm \Delta\delta$	$\delta \pm \Delta\delta$	$\delta \pm \Delta\delta$	$\delta \pm \Delta\delta$
			Real Parts of Phase Shifts		
$^1S_0$	-12.58 1.57	-38.27 4.82	-16.16 1.65	-14.47 1.52	-43.39 6.38
$^3S_1$	5.63 3.25	2.42 4.34	6.73 3.60	38.03 2.70	39.13 4.01
$^3P_0$	-12.65 1.44	-17.60 2.05	-12.11 1.51	-13.27 1.55	-18.89 2.13
$^1P_1$	-43.29 2.50	-37.95 2.37	-33.74 4.12	-22.33 5.28	-20.58 12.74
$^3P_1$	-32.66 0.65	-29.53 1.02	-32.82 0.69	-32.40 0.77	-28.83 1.16
$^3P_2$	18.90 0.39	19.18 0.46	18.93 0.41	18.91 0.43	19.16 0.58
ε_1	-0.65 2.35	-4.27 1.90	16.89 2.34	-26.24 2.25	-13.78 6.98
$^3D_1$	-35.50 2.42	-34.09 2.19	38.63 3.28	31.12 3.60	43.03 3.18
$^1D_2$	13.17 0.30	11.58 0.45	13.27 0.26	13.33 0.28	11.63 0.40
$^3D_2$	11.82 3.44	17.77 2.15	14.49 2.29	9.60 2.01	2.50 6.74
$^3D_3$	-1.74 1.82	-2.15 1.58	5.64 1.60	3.31 1.14	3.05 1.53
ε_2	0.08 0.55	-0.83 0.71	-0.16 0.50	-0.09 0.60	-1.65 0.73
$^3F_2$	0.79 0.40	0.28 0.54	0.47 0.40	0.62 0.39	-0.54 0.59
$^1F_3$	-4.08 1.03	-5.78 0.81	0.12 1.73	-3.89 1.25	-4.14 2.82
$^3F_3$	-1.95 0.40	-2.05 0.49	-0.17 0.38	-1.69 0.41	-1.65 0.54
$^3F_4$	3.37 0.19	3.05 0.20	3.25 0.19	3.36 0.19	2.96 0.21
ε_3	8.01 0.68	9.02 0.60	-5.51 1.40	-0.54 1.79	-0.74 4.86
$^3G_3$	-0.14 1.40	-0.30 1.84	-1.80 1.02	-0.30 1.58	3.60 1.64
$^1G_4$	2.61 0.20	1.95 0.24	2.51 0.20	2.68 0.20	1.67 0.25
$^3G_4$	-1.80 0.82	-1.71 0.94	-3.13 0.87	-2.92 0.87	-2.99 0.74
$^3G_5$	-4.78 1.57	27.04 6.01	-3.46 1.79	-5.14 1.53	36.01 6.79
			Imaginary Part of Phase Shift		
$^1D_2$	4.15 0.85	-0.67 0.55	3.65 0.86	3.97 0.85	-0.95 0.54
f^2	0.083 0.007	0.071 0.007	0.083 0.007	0.093 0.009	0.065 0.013
χ^2	115.67	124.05	138.06	138.27	141.80
$\chi^2/\overline{\chi^2}$	0.91	0.98	1.10	1.10	1.12
Solution	1	2	3	4	5

Table 4

The Phase Shifts in Degrees (the Stapp Parametrization) for 400 MeV Nucleon-Nucleon Scattering ($\ell_{max} = 5$).

Phase Shifts	δ	$\pm \Delta\delta$
	Real Parts	
$^1S_0$	-19.51	1.22
$^3S_1$	- 3.75	23.40
$^3P_0$	-10.21	2.27
$^1P_1$	-37.11	20.71
$^3P_1$	-32.29	1.04
$^3P_2$	19.40	0.94
ε_1	5.28	11.62
$^3D_1$	-30.29	5.94
$^1D_2$	13.18	0.43
$^3D_2$	21.69	11.74
$^3D_3$	-24.71	1.64
ε_2	0.54	0.61
$^3F_2$	0.26	0.54
$^1F_3$	- 4.77	2.90
$^3F_3$	- 1.28	0.57

Phase Shifts	δ	$\pm \Delta\delta$
$^3F_4$	3.13	0.24
ε_3	7.16	3.11
$^3G_3$	-1.46	6.33
$^1G_4$	2.52	0.19
$^3G_4$	7.23	8.56
$^3G_5$	-1.41	1.41
ε_4	-1.92	0.26
$^3H_4$	-0.56	0.63
$^1H_5$	-2.91	1.67
$^3H_5$	-0.80	0.50
$^3H_6$	-0.08	0.43
	Imaginary Part	
$^1D_2$	2.41	0.67
f^2	0.070	0.010
χ^2	113.32	
$\chi^2/\overline{\chi^2}$	0.94	

Table 5

The Distribution Coefficients for the Phase Shift Energy Dependences*)

Phase Shift	a_1x10	Distribution a_2x10^2	Coefficients a_3x10^3	**) a_4x10^4	a_5x10^5	χ^2	$\chi^2/\overline{\chi^2}$
$^1S_0$	- 0.62167	- 50.51601	19.56261	- 1.73342	0.00	7.80	1.10
$^3S_1$	-321.37470	291.15107	-133.75979	22.54389	0.00	35.59	5.00
$^3P_0$	- 21.39313	157.98911	-204.25080	93.23066	-14.37793	4.89	0.70
$^1P_1$	- 17.40493	47.53864	- 50.04244	12.76300	0.00	11.99	1.33
$^3P_1$	- 8.57288	2.43745	- 9.79476	3.33477	0.00	4.51	0.50
$^3P_2$ ***)	0.00	-2.78793	46.21441	-48.46290	17.97259	8.39	1.40
ε_1	- 36.14370	81.47201	- 52.86998	10.65984	0.00	11.70	1.45
$^3D_1$	18.95803	- 47.34628	20.63553	- 2.57192	0.00	27.43	3.14
$^1D_2$	- 4.99527	25.74542	-31.16457	17.37099	- 3.38205	9.44	1.35
$^3D_2$	0.00	0.00	68.61407	-60.91444	13.59093	1.56	0.20
$^3D_3$	- 4.36333	9.96765	- 3.91386	0.00	0.00	8.89	1.11
ε_2	- 1.94010	-1.53039	1.15249	0.00	0.00	3.88	0.97
$^3F_2$	- 0.65337	-2.48530	4.43860	-1.44189	0.00	7.06	2.35
$^1F_3$	3.88930	-13.41809	8.48576	-1.65464	0.00	2.08	0.70
$^3F_3$	3.29351	-6.84631	2.31248	0.00	0.00	1.86	0.62
$^3F_4$ ***)	0.00	0.00	-11.79384	20.64142	-11.00275	3.52	1.76
ε_3	3.19683	0.48349	0.00	0.00	0.00	2.63	1.31
$^3G_3$	- 2.84551	0.92549	0.00	0.00	0.00	4.75	2.37
$^1G_4$	- 0.79857	1.09860	0.00	0.00	0.00	4.51	2.25
$^3G_4$	6.26666	-1.69013	0.00	0.00	0.00	0.004	0.004
$^3G_5$	0.86262	-0.83942	0.00	0.00	0.00	4.85	2.42

*) The distribution coefficients are calculated using the 3-rd set of 630 MeV phase shift analysis.

**) The coefficient a_0 is equal to zero for all phase shifts except $^3S_1$ (a_0 =180°) and $^1S_0$ (a_0 =60.22901°).

***) For the description of the energy dependences of phase shifts $^3P_2$ and $^3F_4$ the coefficient a_6 is used. It is equal to $a_6 \cdot 10$ =-2.17953 and $a_6 \cdot 10^6$ = 1.86752, respectively.

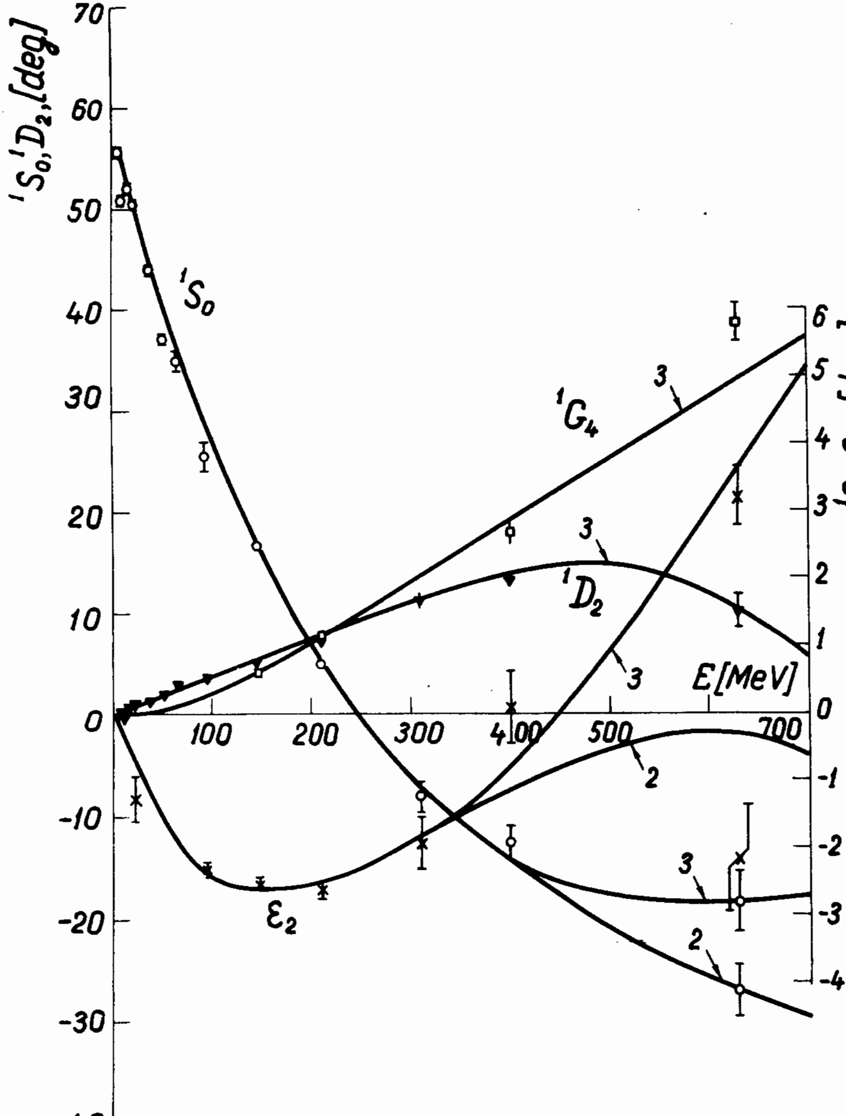

Fig.1. Energy dependences of phase-shifts in 10–700 MeV region. The data $^1S_0$ (14.5, 52 MeV) and $^1D_2$ (14.5 MeV) were not taken into account.

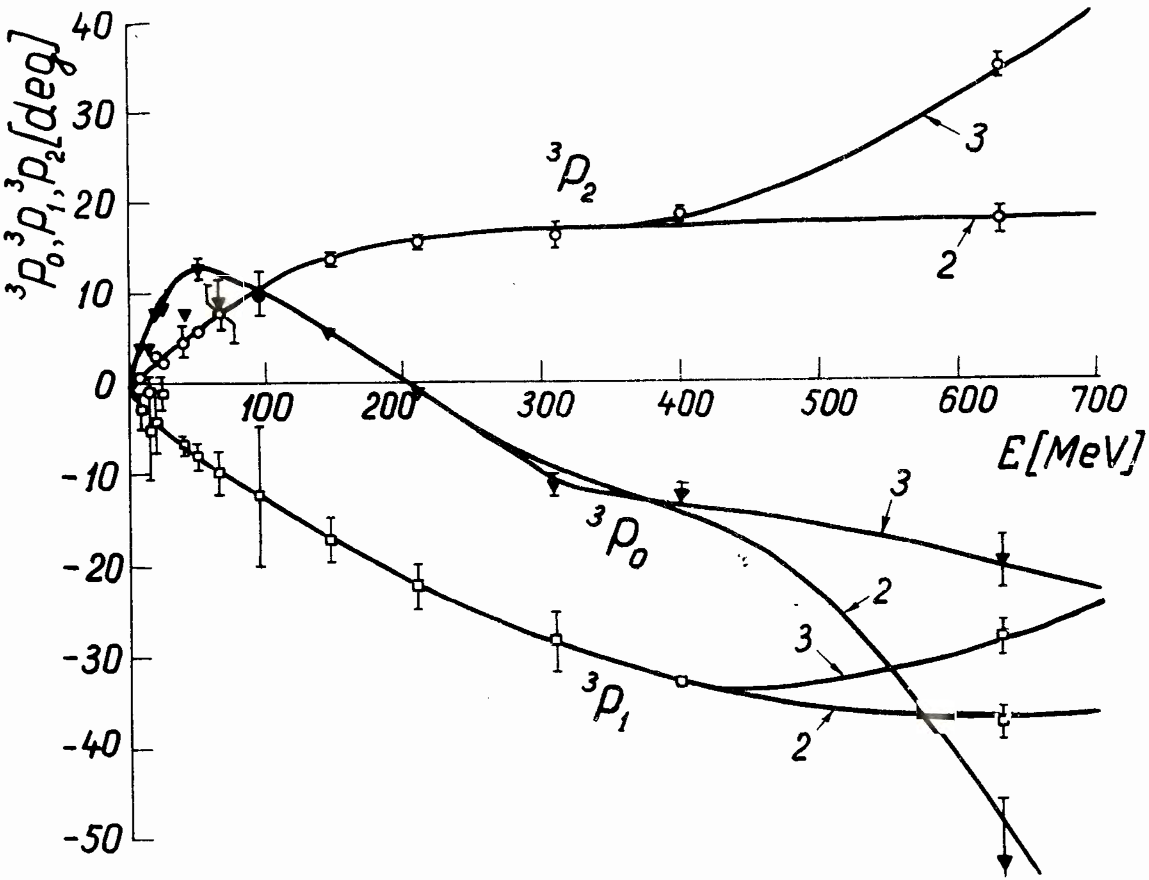

Fig.2. Energy dependences of phase shifts in 10-700 MeV region. The data $^3P_0$ (40 MeV) and $^3P_2$ (14.5, 18.2 MeV) were not taken into account.

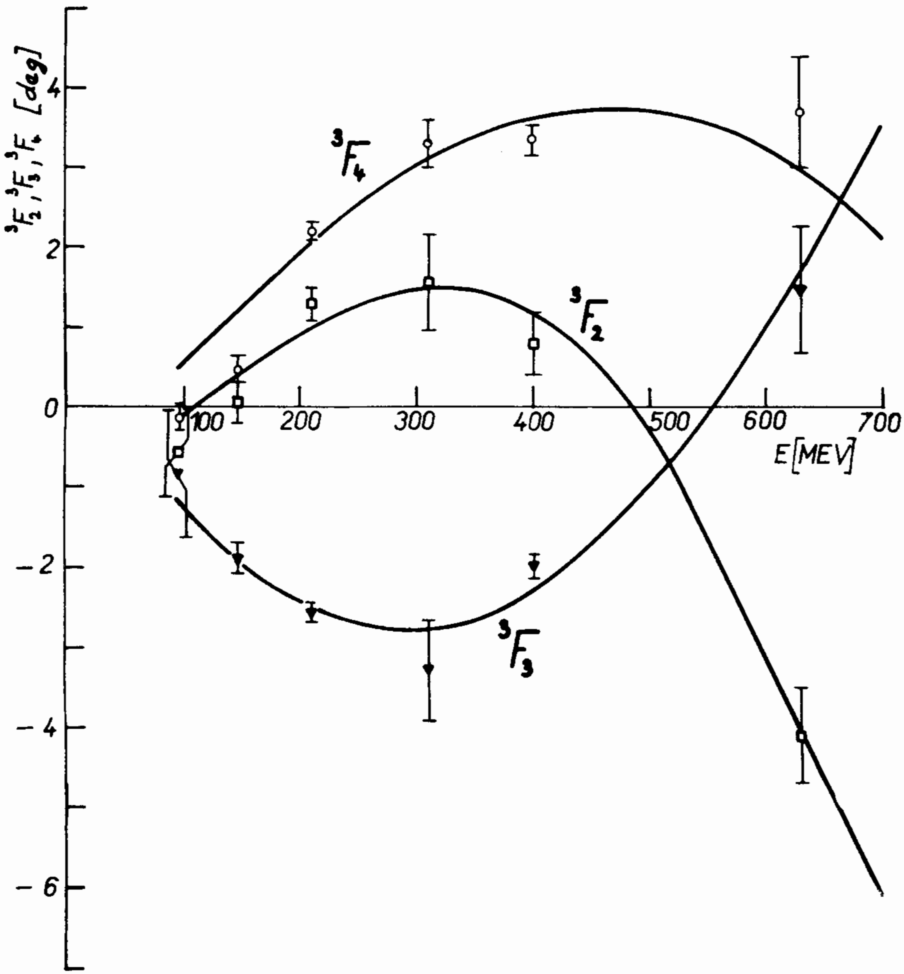

Fig.3. Energy dependences of phase shifts in 100-700 MeV region.

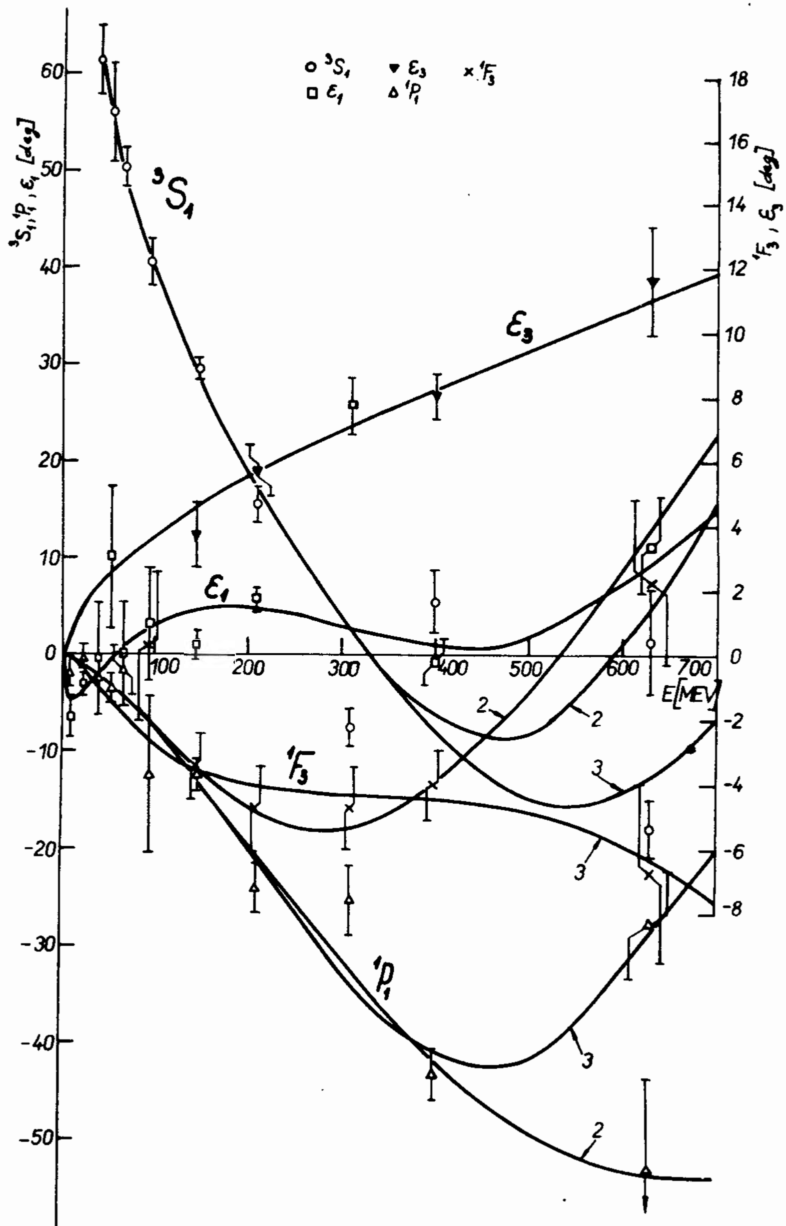

Fig.4. Energy dependences of phase shifts in 10-700 MeV region. The value ϵ_1 (310 MeV) was not taken into account.

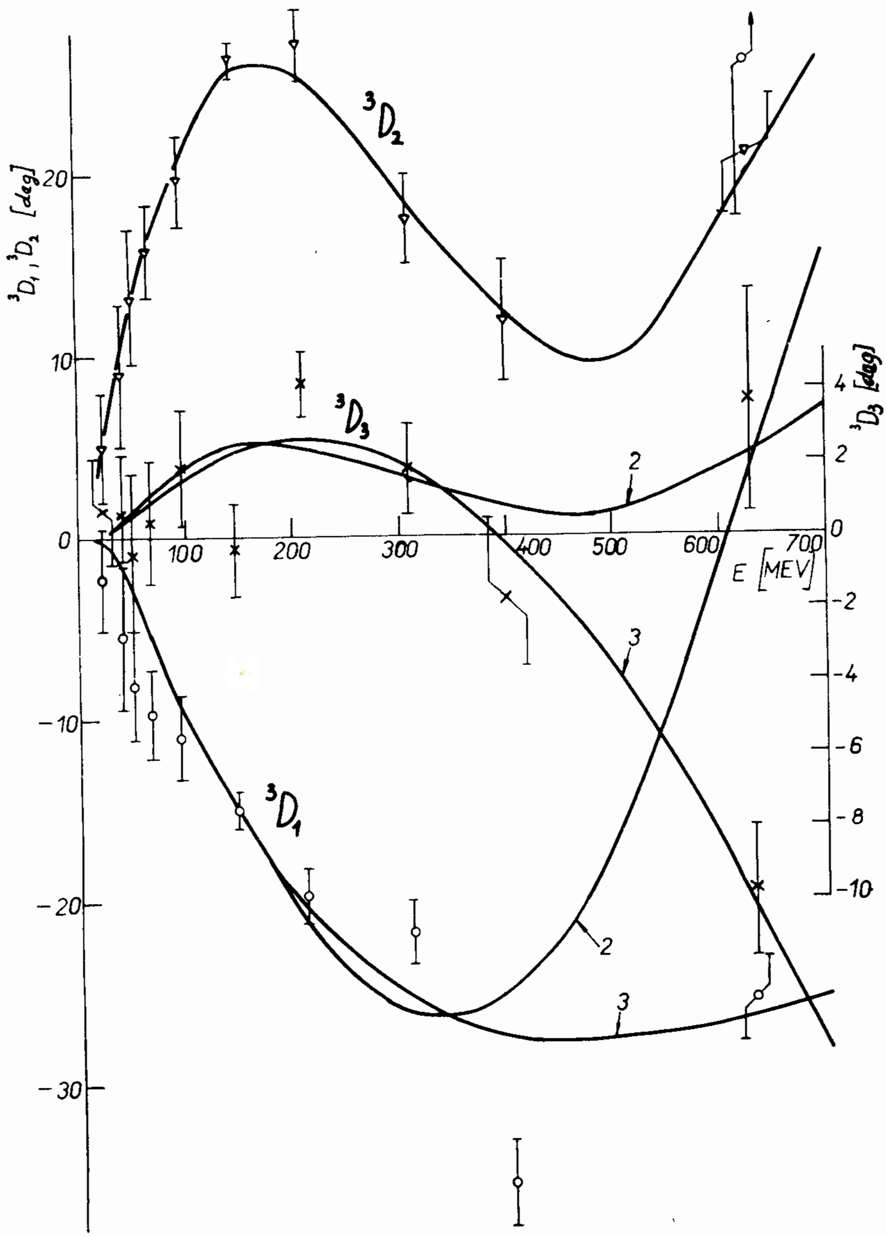

Fig.5. Energy dependences of phase shifts in 20-700 MeV region.

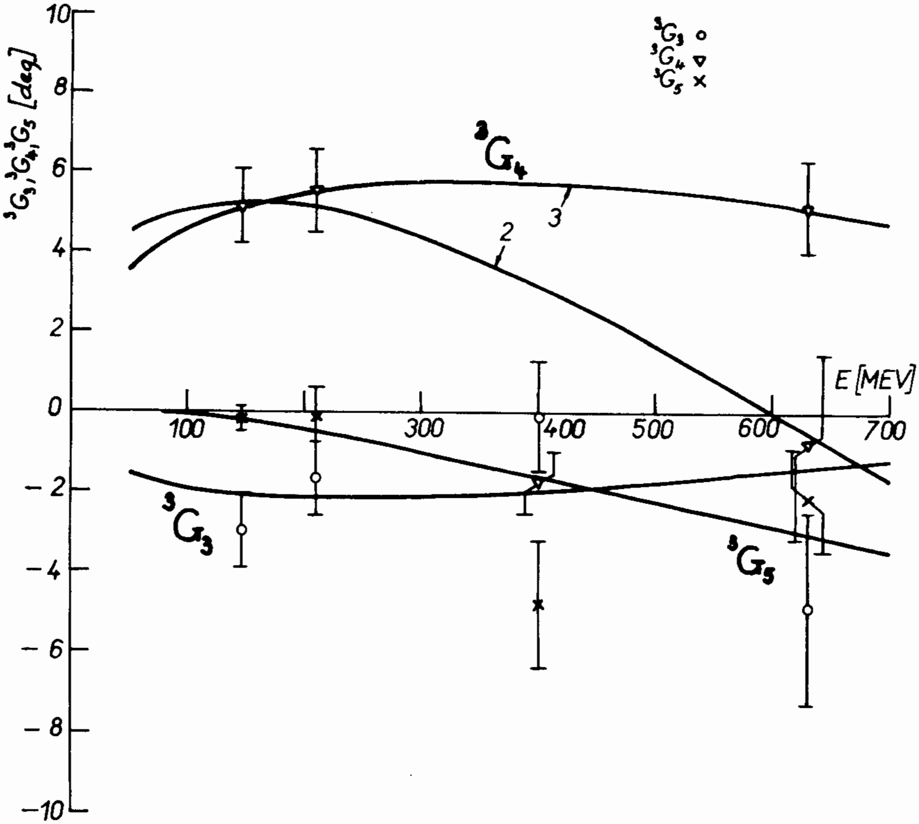

Fig.6. Energy dependences of phase shifts in 100-700 MeV region.

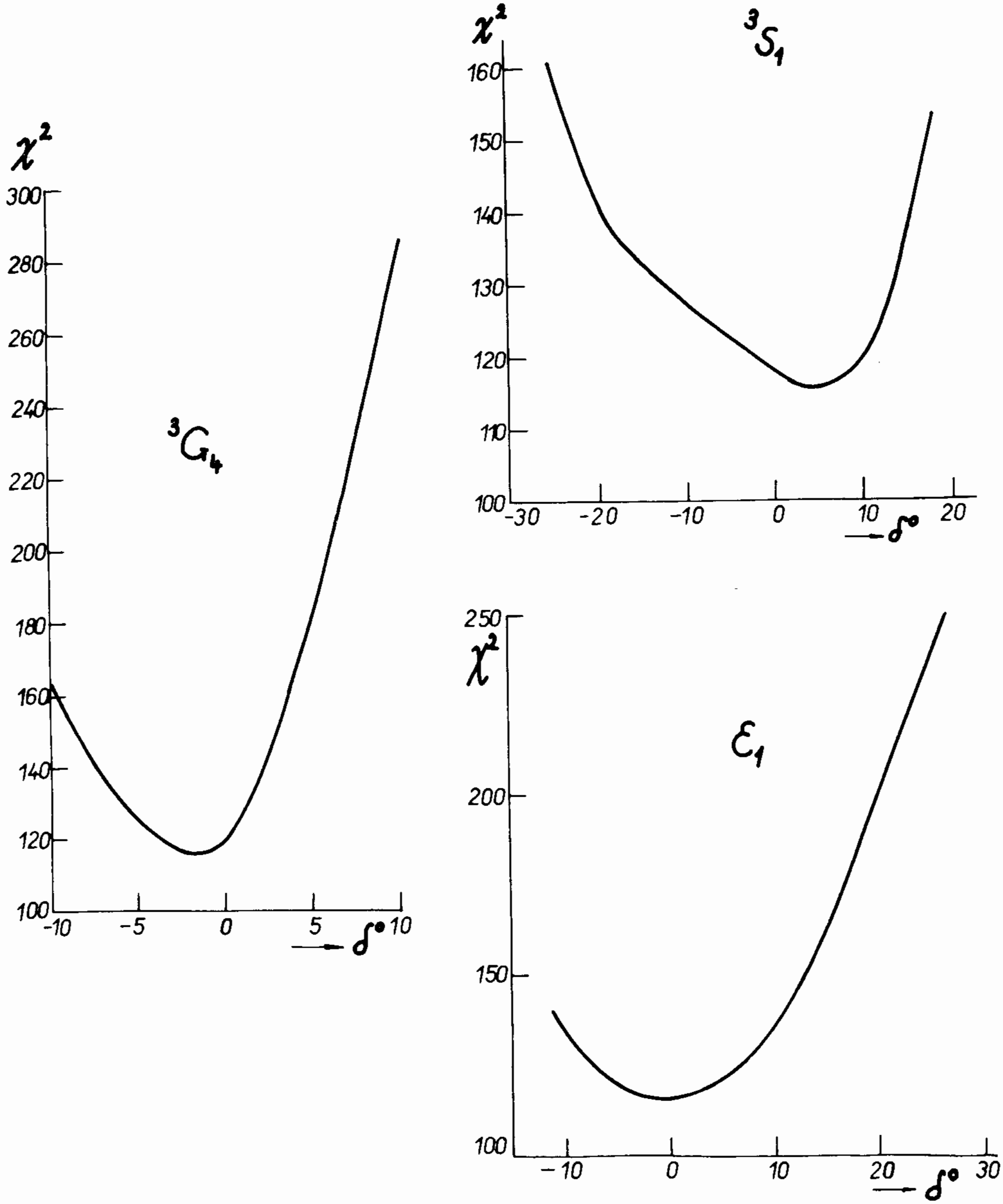

Fig.7. The dependence of χ^2 on $^3S_1$, ϵ_1 $^3G_4$ phase shift values, respectively.

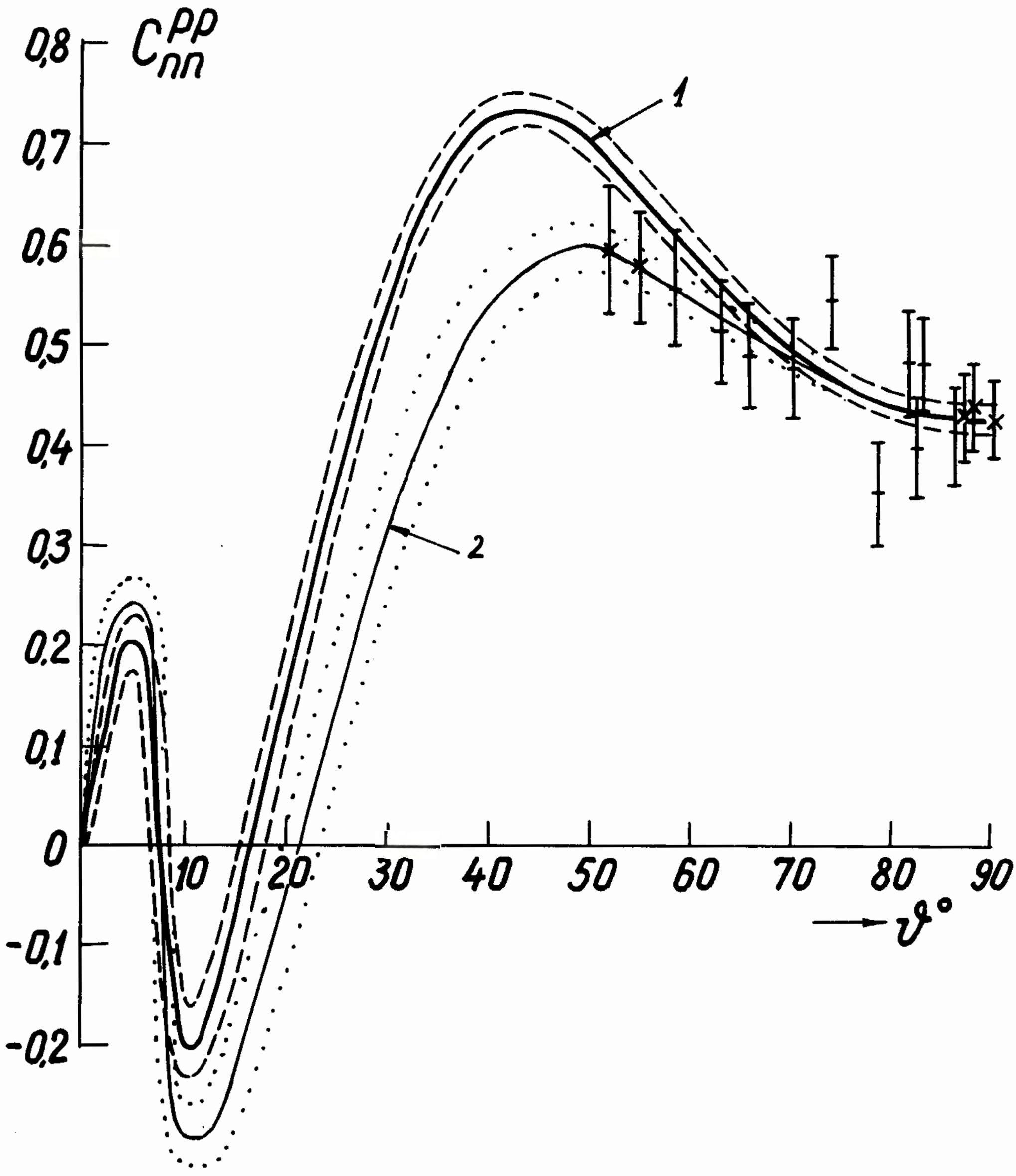

Fig.8. The angular dependence of C_{nn}^{pp} for 1-st and 2-nd phase shift sets. Experimental data are measured by Beretvas et al. /3/.

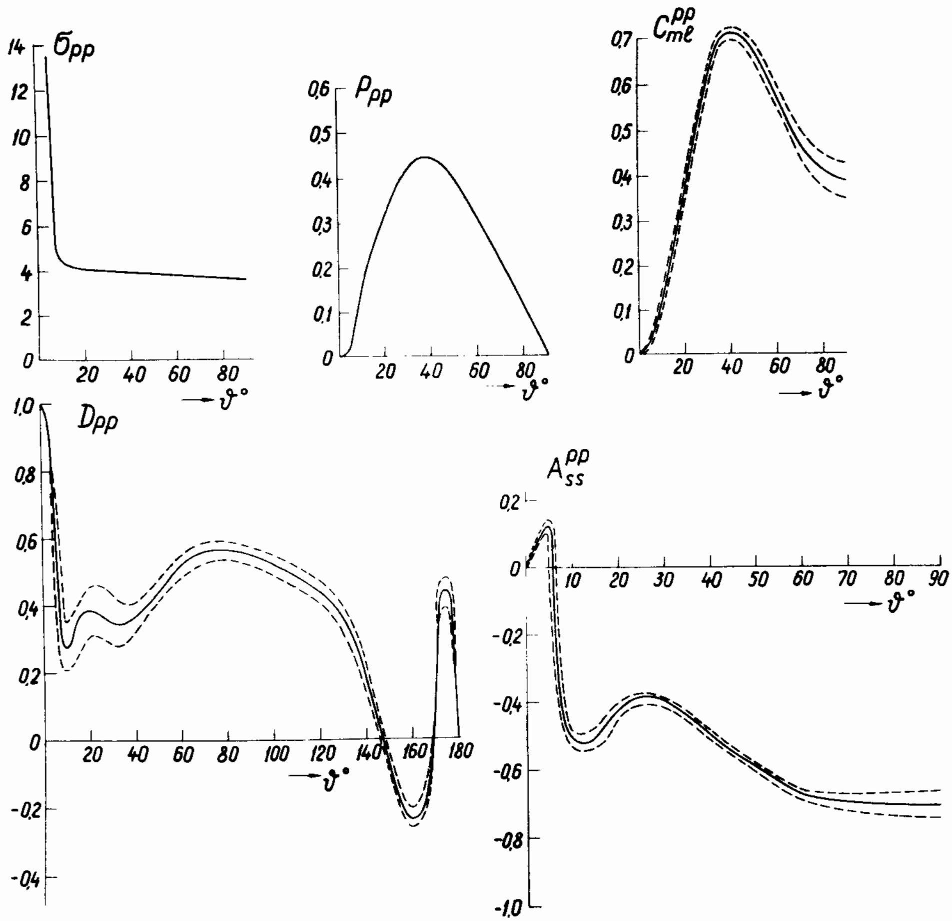

σpp
14
12
10
8
6
4
2
0
20
40
60
80
ϑ°
Ppp
0,6
0,5
0,4
0,3
0,2
0,1
0
20
40
60
80
ϑ°
C_{ml}^{pp}
0,7
0,6
0,5
0,4
0,3
0,2
0,1
0
20
40
60
80
ϑ°
Dpp
1,0
0,8
0,6
0,4
0,2
0
-0,2
-0,4
20
40
60
80
100
120
140
160
180
ϑ°
A_{ss}^{pp}
0,2
0
-0,2
-0,4
-0,6
-0,8
-1,0
10
20
30
40
50
60
70
80
90
ϑ°

Fig. 9.

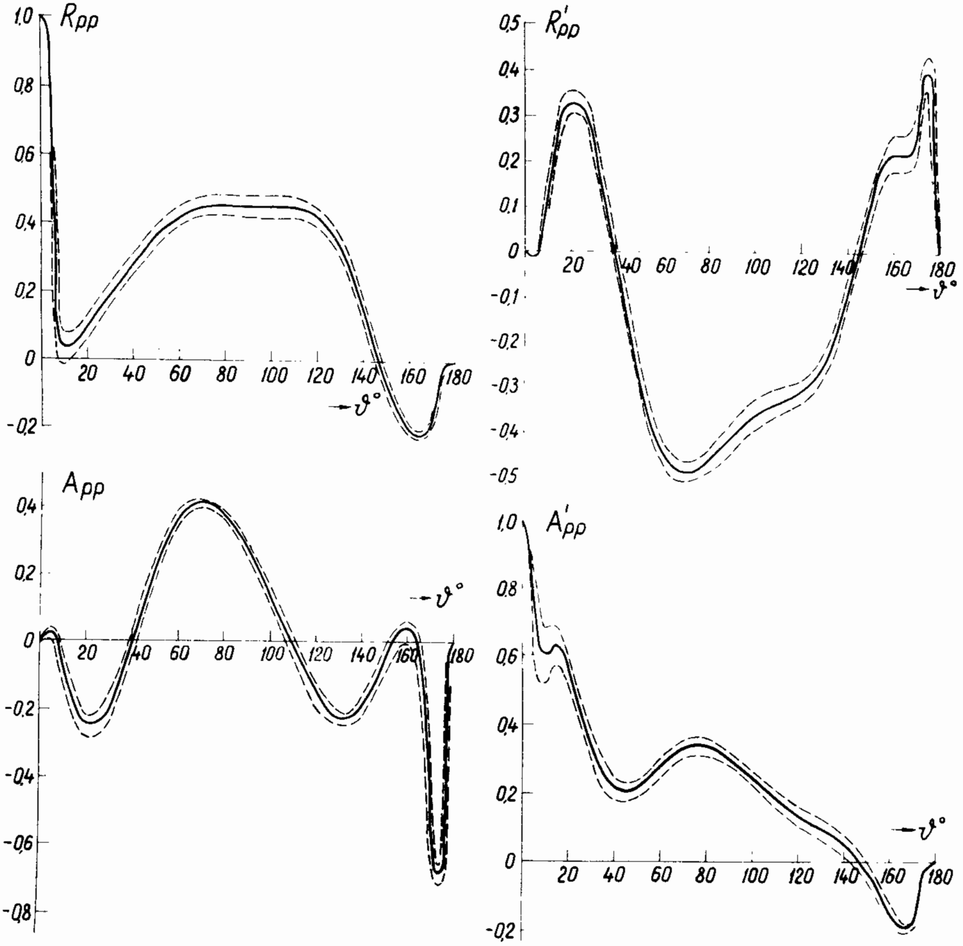

Fig.10.

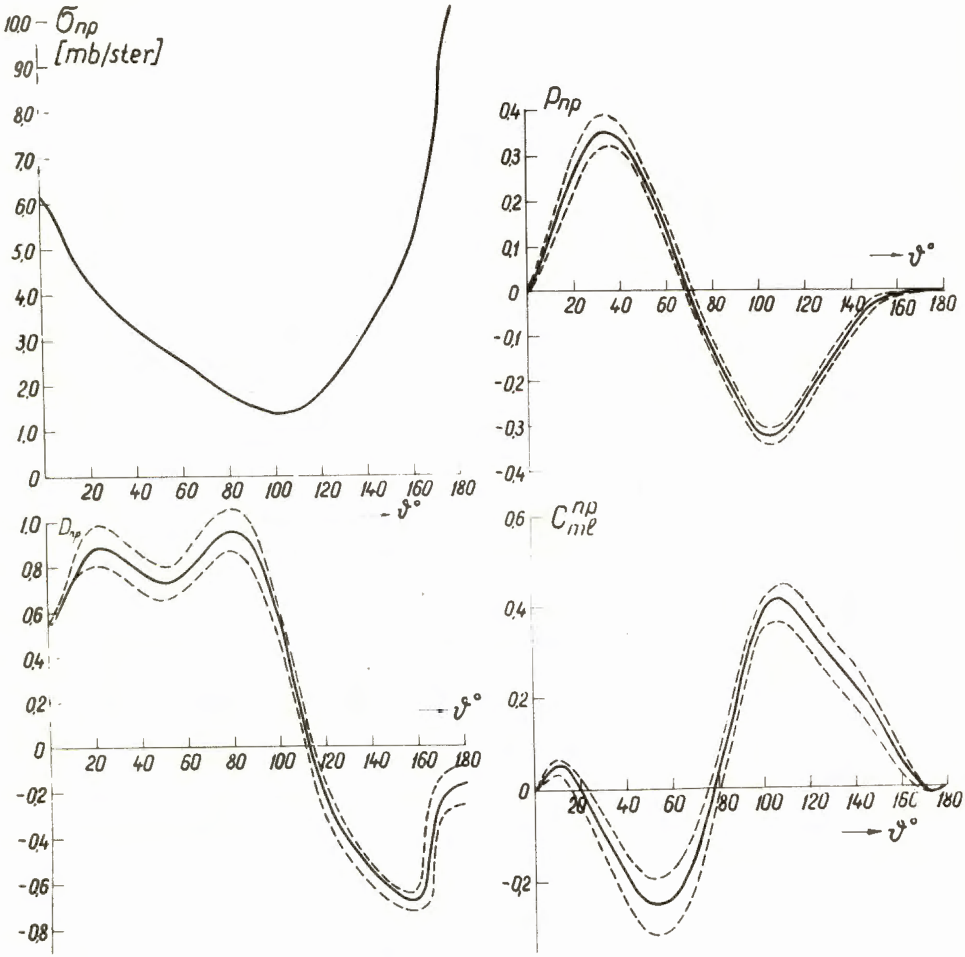

100
90
80
70
60
50
40
30
20
10
0
20
40
60
80
100
120
140
160
180
[mb/ster]
0,4
0,3
0,2
0,1
0
-0,1
-0,2
-0,3
-0,4
1,0
0,8
0,6
0,4
0,2
-0,2
-0,4
-0,6
-0,8
0,6

Fig.11.

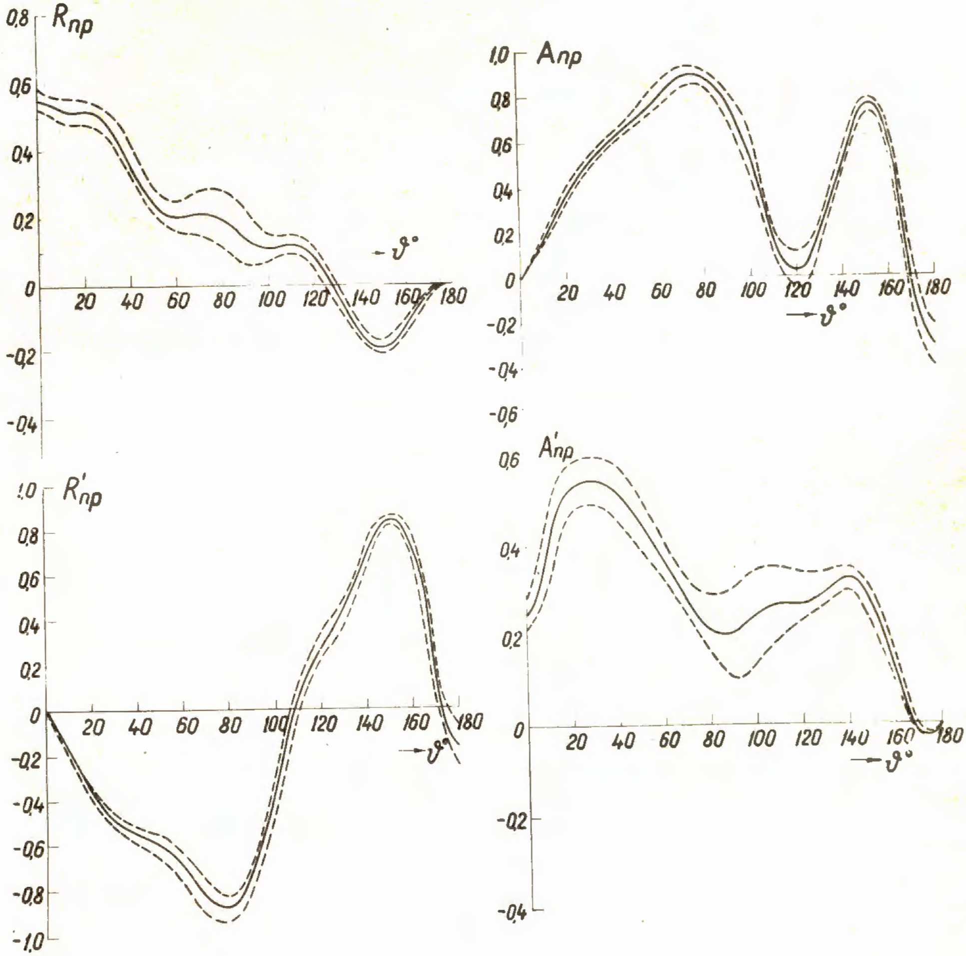

Fig.12.

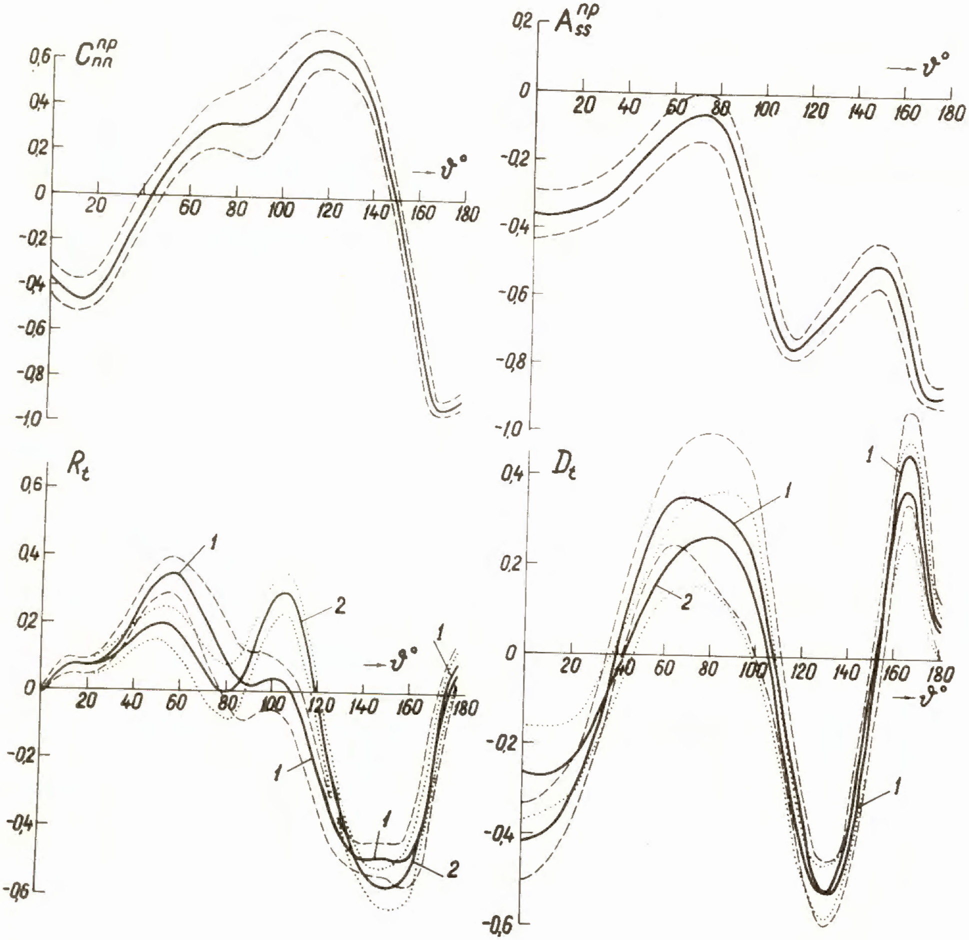

Fig. 13.